Reproductive Sciences (2020) 27:2092–2103
https://doi.org/10.1007/s43032-020-00230-6

GYNECOLOGIC ONCOLOGY: ORIGINAL ARTICLE

Possibility of Targeting Claudin-2 in Therapy for Human Endometrioid Endometrial Carcinoma

Tadahi Okada[1,2] · Takumi Konno[1] · Takayuki Kohno[1] · Hiroshi Shimada[2] · Kimihito Saito[1,2] · Seiro Satohisa[2] · Tsuyoshi Saito[2] · Takashi Kojima[1]

Received: 18 February 2020 / Revised: 24 May 2020 / Accepted: 2 June 2020 / Published online: 16 June 2020

Abstract

Claudin-2 (CLDN-2) is a leaky-type tight junction protein, and its overexpression increases tumorigenesis of some types of cancer cells. In the present study, to examine the possibility of targeting CLDN-2 in the therapy for endometrioid endometrial adenocarcinoma, we investigated the regulation and role of CLDN-2 in endometriosis and endometrioid endometrial adenocarcinoma. In endometrioid endometrial adenocarcinoma tissues, marked upregulation of CLDN-2 was observed together with malignancy, while in endometriosis tissues, a change in the localization of CLDN-2 was observed. In cells of the endometrial adenocarcinoma cell line Sawano, which highly express CLDN-2, downregulation of CLDN-2 induced by the siRNA upregulated the epithelial barrier and inhibited cell migration. Furthermore, the downregulation of CLDN-2 affected the cell cycle and inhibited cell proliferation. In Sawano cells cultured with high-glucose medium, CLDN-2 expression was downregulated at the mRNA and protein levels. The high-glucose medium upregulated the epithelial barrier, cell proliferation, and migration, and inhibited cell invasion. The histone deacetylase (HDAC) inhibitor tricostatin A (TSA), which has antitumor effects, downregulated CLDN-2 expression, cell proliferation, invasion, and migration, and upregulated the epithelial barrier. The mitochondrial respiration level, an indicator of cancer metabolism, was downregulated by CLDN-2 knockdown and upregulated by the high-glucose condition. Taken together, these results indicated that overexpression of CLDN-2 closely contributed to the malignancy of endometrioid endometrial adenocarcinoma. Downregulation of CLDN-2 via the changes of the glucose concentration and treatment with HDAC inhibitors may be important in the therapy for endometrial cancer.

Keywords Claudin-2 · Malignancy · Human endometrioid endometrial carcinoma · High glucose · HDAC inhibitor · Cancer metabolism

Introduction

Endometrial cancer was the sixth most commonly diagnosed cancer and the 14th leading cause of cancer death in women worldwide in 2012 [1]. Its incidence has increased over time and in successive generations in half of the population, especially in those countries with rapid socioeconomic transitions [2]. Therefore, further elucidation of the pathophysiology of endometrial cancer is needed to develop new treatments.

The tight junction (TJ) is an epithelial cell-cell junction that regulates the flow of solutes through paracellular pathways and maintains cell polarity [3, 4]. TJs are also involved in signal transduction mechanisms that regulate epithelial cell proliferation, gene expression, differentiation, and morphogenesis [5]. Claudins are major components of TJs, which have four transmembrane domains and molecular masses of 20–27 kDa [6, 7]. Claudins constitute a family of over 20 members in mammals, and their subtypes form homo- and heterotypic associations with each other [8, 9]. The overexpression of certain TJ proteins, including CLDNs, is associated with tumor growth and metastasis [10]. The upregulation of

Tadahi Okada and Takumi Konno are equal first authors.

Electronic supplementary material The online version of this article (https://doi.org/10.1007/s43032-020-00230-6) contains supplementary material, which is available to authorized users.

✉ Takashi Kojima
ktakashi@sapmed.ac.jp

[1] Department of Cell Science, Research Institute for Frontier Medicine, Sapporo Medical University School of Medicine, South-1, West-17, Chuo-ku, Sapporo 060-8556, Japan

[2] Department of Obstetrics and Gynecology, Sapporo Medical University School of Medicine, Sapporo, Japan

claudin-2 (CLDN-2) expression in human lung, liver, colon, and stomach cancer tissues is reported [11–14]. In human lung adenocarcinoma cells, nuclear distribution of CLDN-2 increases cell proliferation, and CLDN-2 knockdown decreases matrix metalloproteinase-9 activity and cell migration via suppression of nuclear Sp1 [15, 16]. Moreover, overexpression of CLDN-2 in weakly aggressive breast cancer cells increases liver metastasis [17]. Based on these reports, it is considered that claudin-2 may be involved in the malignancy of cancer tissues.

The relation between diabetes and endometrial cancer is controversial [18]. It is reported that diabetes may contribute to cancer progression [19]. In type 2 diabetes, there is high plasma glucose concentration [18]. A high glucose level promotes epithelial-mesenchymal transition (EMT) of uterine endometrial cancer cells by increasing ER/GLUT4-mediated VEGF secretion [20]. It is reported that the high-glucose condition modulates tight junction-associated epithelial barrier function in a renal tubular cell line [21]. In that report, immunofluorescence analyses showed that glucose treatment induced a significant decrease in the tight junctional content of CLDN-1 and CLDN-3 as well as a significant increase in CLDN-2 [21]. In normal human endometrium, expression of claudin-1, claudin-2, claudin-3, claudin-4, claudin-5, claudin-7, and claudin-10 is detected and expression of claudin-2, claudin-3, and claudin-4 is similarly abundant throughout the menstrual cycle [22, 23]. Localization of claudin-2 is highly stable in eutopic and ectopic endometrium [24]. In human endometrial cancer, CLDN-2 is elevated in type I endometrioid endometrial carcinoma, while overexpression of CLDN-1 is observed in type II seropapillary endometrial carcinoma [22, 23]. However, the roles of CLDNs with regard to the malignancy in endometrial cancer cells remain unknown.

In cancer, several alterations of mitochondrial DNA (mtDNA) such as deletions, point mutations, and copy number variations cause mitochondrial dysfunction [25]. It is thought that mitochondrial dysfunction may be a novel potential driver of epithelial-to-mesenchymal transition (EMT) in cancer [26]. Mitochondrial dysfunction of type I endometrioid endometrial carcinoma contributes to tumor progression and prognosis [27]. There is a close interaction between mitochondria homeostasis and epithelial cell homeostasis, and mitochondrial dysfunction also contributes to altered barrier permeability [28]. The effects of tight junctions including CLDNs in mitochondria homeostasis during the malignancy of cancer cells are still unclear.

On the other hand, HDAC inhibitors induce differentiation, growth arrest, and apoptosis in cancer cells [29, 30]. In human endometrial cancer, HDAC inhibitors may also become a new therapeutic target [29]. It is reported that trichostatin A (TSA), an HDAC inhibitor, attenuates invasiveness and reactivates E-cadherin expression in immortalized endometriotic cells [30]. It is also reported that TSA decreases the stability of CLDN-2 and suppresses proliferation of human lung adenocarcinoma cells [31].

Endometrioid adenocarcinoma arising from endometriosis is rare in premenopausal woman [32]. In this study, to examine the possibility of targeting CLDN-2 in therapy for endometrioid endometrial adenocarcinoma, we investigated the regulation and the role of CLDN-2 in endometrioid endometrial adenocarcinoma and endometriosis. Furthermore, we analyzed the role of CLDN-2 in cancer metabolism.

Materials and Methods

Reagents and Antibodies

Trichostatin A (TSA) was purchased from Abcam (Cambridge, UK). Cycloheximide (CHX) was purchased from Nacalai Tesque (Kyoto, Japan). A rabbit polyclonal anti-claudin (CLDN)-2 antibody and a mouse monoclonal anti-CLDN-2 antibody were obtained from Zymed Laboratories (San Francisco, CA, USA). A mouse monoclonal anti-acetylated tubulin antibody and a rabbit polyclonal anti-actin antibody were from Sigma-Aldrich (St. Louis, MO, USA). Alexa 488 (green)-conjugated anti-rabbit IgG and Alexa 594 (red)-conjugated anti-mouse IgG antibodies and Alexa 594 (red)-conjugated phalloidin were from Molecular Probes, Inc. (Eugene, OR). HRP-conjugated polyclonal goat anti-rabbit IgG was from Dako A/S (Glostrup, Denmark). The ECL Western blotting system was from GE Healthcare UK, Ltd. (Buckinghamshire, UK).

Immunohistochemical (IHC) Analysis

Human endometrial carcinoma tissues and human endometrial tissues were obtained from 6 patients with endometriosis and 15 patients with endometrioid endometrial adenocarcinoma (G1: 7, G2: 4, and G3: 4) who underwent hysterectomy at Sapporo Medical University Hospital. Written informed consent was obtained from all patients. The study was approved by the ethics committee of Sapporo Medical University. Hematoxylin and eosin-stained slides from each case were reviewed, and the diagnoses and grades of the tumors were determined according to the WHO classification. The diagnoses of endometriosis and endometrial adenocarcinoma were established by both gynecologists and pathologists. All endometrial adenocarcinomas were the classic endometrial type I.

Human endometriosis and endometrial cancer tissues were embedded in paraffin after fixation with 10% formalin in PBS. Briefly, 5-μm-thick sections were dewaxed in xylene, rehydrated in ethanol, and heated with Vision BioSystems Bond Max using ER2 solution (Leica) in an autoclave for antigen retrieval. Endogenous peroxidase was blocked by

incubation with 3% hydrogen peroxide in methanol for 10 min. The tissue sections were then washed twice with Tris-buffered saline (TBS) and preblocked with Block Ace for 1 h. After washing with TBS, the sections were incubated with a mouse monoclonal anti-CLDN-2 (1:100) antibody for 1 h. Negative controls were prepared by omission of the primary antibody. The sections were then washed three times in TBS and incubated with Vision BioSystems Bond Polymer Refine Detection kit DS9800. After three washes in TBS, a diamino-benzidine tetrahydrochloride working solution was applied. Finally, the sections were counterstained with hematoxylin. IHC quantification was done by use of the H-score. The extent of positively stained area was scored from 0 to 3 according to the percentage of atypical cells showing positive IHC staining: 0 (0%), 1 (1–25%), 2 (26–50%), and 3 (51–100%). The intensity of staining was graded 0 to 3 according to the intensity of IHC staining: 0 (none), 1 (weak), 2 (moderate), and 3 (strong). H-score (0–300) = (% cells not stained × 0) + (% cells stained weak × 1) + (% cells stained moderate × 2) + (% cells stained strong × 3).

Cell Line Culture and Treatment

The human endometrioid endometrial cancer cell line Sawano (RCB1152) was purchased from RIKEN Bio-Resource Center (Tsukuba, Japan). The cells were maintained with minimum essential medium (MEM, Nacalai Tesque, Inc.; Kyoto, Japan) supplemented with 10% dialyzed fetal bovine serum (FBS; Invitrogen, Carlsbad, CA, USA). The medium contained 100 U/ml penicillin, 100 μg/ml streptomycin, and 50 μg/ml amphotericin-B. Sawano cells were plated on 35- and 60-mm culture dishes, which were coated with rat tail collagen (500 μg dried tendon/ml in 0.1% acetic acid), and incubated in a humidified 5% CO_2 incubator at 37 °C. Some cells were cultured with high-glucose medium (Dulbecco's modified Eagle's medium (DMEM), with 4500 mg/ml glucose, Nacalai Tesque, Inc., Kyoto, Japan) and treated with 1 or 10 μg/ml TSA. Furthermore, in the presence of 50 μM cycloheximide, a translation inhibitor, the protein levels of CLDN-2 were measured in a time-dependent manner.

RNA Interference and Transfection

siRNA duplex oligonucleotides against CLDN-2 were synthesized by Santa Cruz Biotechnology (Dallas, TX). The sequences were as follows: siRNA of CLDN-2A (sc37457, sense: 5′-CUAGAAGCCUUACGAAAGAtt-3′; antisense: 5′-UCUUUCGUAAGGCUUCUAGtt-3′), siRNA of CLDN-2B (sc37457, sense: 5′-CCAUCUCUGUCCCAUCAUAtt-3′; antisense: 5′-UAUGAUGGGACAGAGAUGGtt-3′). At 24 h after plating, the Sawano cells were transfected with 100 nM siRNAs of CLDN-2(A, B) using Lipofectamine™ RNAiMAX Reagent (Invitrogen) for 48 h. A scrambled siRNA sequence (BLOCK-iT Alexa Fluor Fluorescent, Invitrogen) was employed as control siRNA.

Immunocytochemical Staining

Sawano cells in 35-mm glass-coated wells (Iwaki, Chiba, Japan) were fixed with cold acetone and ethanol (1:1) at − 20 °C for 10 min. After rinsing in PBS, the cells were incubated with mouse monoclonal anti-CLDN-2 and mouse monoclonal anti-acetylated tubulin antibodies (1:100) overnight at 4 °C. Alexa Fluor 488 (green)-conjugated anti-rabbit IgG and Alexa Fluor 594 (red)-conjugated anti-mouse IgG (Invitrogen) were used as secondary antibodies. The specimens were examined and photographed with an Olympus IX 71 inverted microscope (Olympus Co.; Tokyo, Japan) and a confocal laser scanning microscope (LSM510; Carl Zeiss, Jena, Germany).

RNA Isolation and RT-PCR Analysis

Total RNA was extracted and purified using TRIzol (Invitrogen, Carlsbad, CA). Total RNA (1 μg) was reverse-transcribed into cDNA using a mixture of oligo (dT) and Superscript IV reverse transcriptase according to the manufacturer's recommendations (Invitrogen). Synthesis of each cDNA was first performed by incubation for 5 min at 65 °C and terminated by incubation for 10 min at 80 °C in a total volume 20 μl. The polymerase chain reaction (PCR) was performed in a 20-μl mixture containing 100 pM primer pairs, 1.0 μl of the 20-μl total reverse transcription (RT) product, PCR buffer, dNTPs, and Taq DNA polymerase according to the manufacturer's recommendations (Takara, Kyoto, Japan). Amplifications were carried out for 25–40 cycles depending on the PCR primer pair with cycle times of 15 s at 96 °C, 30 s at 55 °C, and 60 s at 72 °C. The final elongation time was 7 min at 72 °C. Of the total 20-μl PCR product, 7 μl was analyzed by 1% agarose gel electrophoresis with ethidium bromide staining and standardized using a GeneRuler 100-bp DNA ladder (Fermentas, Ontario, Canada). The PCR primers used for CLDN-2 and glucose-3-phosphate dehydrogenase (G3PDH) by RT-PCR had the following sequences: CLDN-2 (sense: 5′-CAAATGCTGCTCATGGAAAGA-3′; antisense: 5′-CAGGACCCAGAGGTGTAGGA-3′) and G3PDH (sense 5′-ACCACAGTCCATGCCATCAC-3′; antisense 5′-TCCACCACCCTGTTGCTGTA-3′).

Western Blot Analysis

The cultured cells were scraped from 60-mm dishes containing 400 μl of buffer (1 mM $NaHCO^3$ and 2 mM phenylmethylsulfonyl fluoride), collected in microcentrifuge tubes, and then sonicated for 10 s. The protein concentrations of the samples were determined using a BCA protein assay

regent kit (Pierce Chemical Co.; Rockford, IL, USA). Aliquots of 15 μl of protein/lane for each sample were separated by electrophoresis in 5–20% SDS polyacrylamide gels (Wako, Osaka, Japan), and electrophoretically transferred to a nitrocellulose membrane (Immobilon; Millipore Co.; Bedford, UK). The membrane was saturated with blocking buffer (25 mM Tris, pH 8.0, 125 mM NaCl, 0.1% Tween 20, and 4% skim milk) for 30 min at room temperature and incubated with rabbit polyclonal anti-CLDN-2 and rabbit polyclonal anti-actin antibodies (1:1000) at room temperature overnight. Then it was incubated with HRP-conjugated anti-mouse and anti-rabbit IgG antibodies at room temperature for 1 h. The immunoreactive bands were detected using an ECL Western blotting system.

Flow Cytometry

Fibroblasts were incubated at 37 °C in Dulbecco's modified Eagle's medium (Thermo Fisher Scientific) containing 10% FBS, stimulated with cytokines for 48 h, harvested, gently centrifuged for 3 min at 1200 rpm, washed in PBS, slowly resuspended in 1 ml of ice-cold 70% ethanol, and stored for 3 h at − 30 °C. After removing the ethanol, the fibroblasts were suspended in 1 ml PBS, centrifuged for 3 min at 1200 rpm, and resuspended in 500 μl PBS, of which 100 μl was stained for 30 min at room temperature in the dark with 100 μl of Muse Cell Cycle Reagent, transferred to a 1.5-ml microcentrifuge tube, and assayed for cell cycle distribution on a Muse Cell Analyzer (Merck, Millipore, Billerica, MA).

Matrigel Invasion Assay

For the invasion assay, we used Matrigel (Becton Dickinson Labware, Bedford, MA) and Cell Culture Insert (pore size 8 μm; Becton Dickinson Labware). Sawano cells were plated onto the upper chamber coated with Matrigel, and the lower chamber of the Transwell was filled with human fibroblast-conditioned medium containing 10 nM EGF as an adhesive substrate. Then the cells were incubated for 36 h, after which the upper chamber was fixed with 100% methanol for 10 min and stained with Giemsa for 20 min. The areas of invading cells were measured using a microscope imaging system (Olympus, Tokyo, Japan).

Migration Assay

After the Sawano cells were plated onto 35-mm dishes, they were cultured to confluence. At 24 h we wounded the cell layer using a plastic pipette tip (P200) and measured the length of the wound by using a microscope imaging system (Olympus, Tokyo, Japan).

XF96 Extracellular Flux Measurements

Mitochondrial respiration was assessed using an XF96 Extracellular Flux Analyzer (Aligent, Santa Clara, CA). Sawano cells were seeded on XF96 plates at a density of 20,000 cells/well after incubation in DMEM medium with high-glucose or glucose-free medium for 24 h. One day prior to the experiment, sensor cartridges were hydrated with XF calibrate solution (pH 7.4) and incubated at 37 °C in a non-CO_2 incubator for 24 h. Baseline measurements of mitochondrial respiration (OCR) were taken before sequential injection of the following inhibitors: 1 μM oligomycin, which is an ATP synthase inhibitor; 2 μM FCCP, which is a mitochondrial respiration uncoupler; and 1 μM antimycin A and rotenone, which are mitochondrial electron transport chain blockers. Oligomycin was applied first to estimate the proportion of basal OCR coupled to ATP synthesis. After oligomycin application, FCCP was used to further determine the maximal glycolysis pathway capacity.

GeneChip Analysis

Microarray slides were scanned using a 3D-GENE human Oligochip 25 k (TORAY, Kamakura, Japan), and microarray images were automatically analyzed using AROSTM, version 4.0 (Operon Biotechnologies, Tokyo, Japan).

Data Analysis

Each set of results shown is representative of at least three separate experiments. Results are given as means ± SEM. Differences between groups were tested by ANOVA followed by a post hoc test and an unpaired two-tailed Student's *t* test.

Results

Expression and Localization of CLDN-2 in Endometriosis and Endometrioid Endometrial Carcinoma

To investigate the distribution and expression of CLDN-2 during the carcinogenesis of human endometrial cancer, immunohistochemical staining for CLDN-2 was performed using paraffin-embedded sections of endometriosis (EM) and endometrioid endometrial carcinoma tissues (G1, G2, G3). We indicated comparison of localization of claudin-2 in the tissues of human normal, endometriosis, and endometrioid endometrial adenocarcinoma by H-score (Table 1). In normal lesions (normal-2), endometriosis (EM-2), and endometrial carcinoma G1 (7/7) and G3 (4/4), CLDN-2 was observed not only in the subapical region but also throughout the lateral region, while it was expressed in the subapical region of some

Table 1 Comparison of localization of claudin-2 in the tissues of human normal, endometriosis, and endometrioid endometrial adenocarcinoma by H-score

	Normal	Endometriosis	Endometrioid endometrial adenocarcinoma		
			G1	G2	G3
Claudin-2					
N	8	6	7	4	4
Mean	135	168	210	225	257
SEM	±25	±32	±28	±30	±22

normal lesions (normal-1) and endometriosis (EM-1) (Fig. 1). CLDN-2 expression increased in the cytoplasma of G3 (4/4) endometrioid endometrial carcinoma compared to G1 (7/7) (Fig. 1).

Loss of CLDN-2 Upregulates Barrier Function and Induces G1 Arrest in Sawano Cells

To investigate how loss of CLDN-2 affected the barrier function and cell cycle in endometrial cancer, we performed knockdown of CLDN-2 by using siRNAs of CLDN-2A and CLDN-2B in human endometrial cancer cell line Sawano. Downregulation of CLDN-2 was shown by siRNAs of CLDN-2A and CLDN-2B in Western blotting (Fig. 2a). In immunocytochemical analysis, CLDN-2 disappeared at the membrane after knockdown by siRNA of CLDN-2B (Fig. 2b). The values of TEER indicated as epithelial barrier function were increased by siRNAs of CLDN-2A and CLDN-2B (Fig. 2c). In the cell cycle assay, an increase of the G0/G1 phase and decreases of the S and G2/M phases were caused by siRNA of CLDN-2B (Fig. 2d).

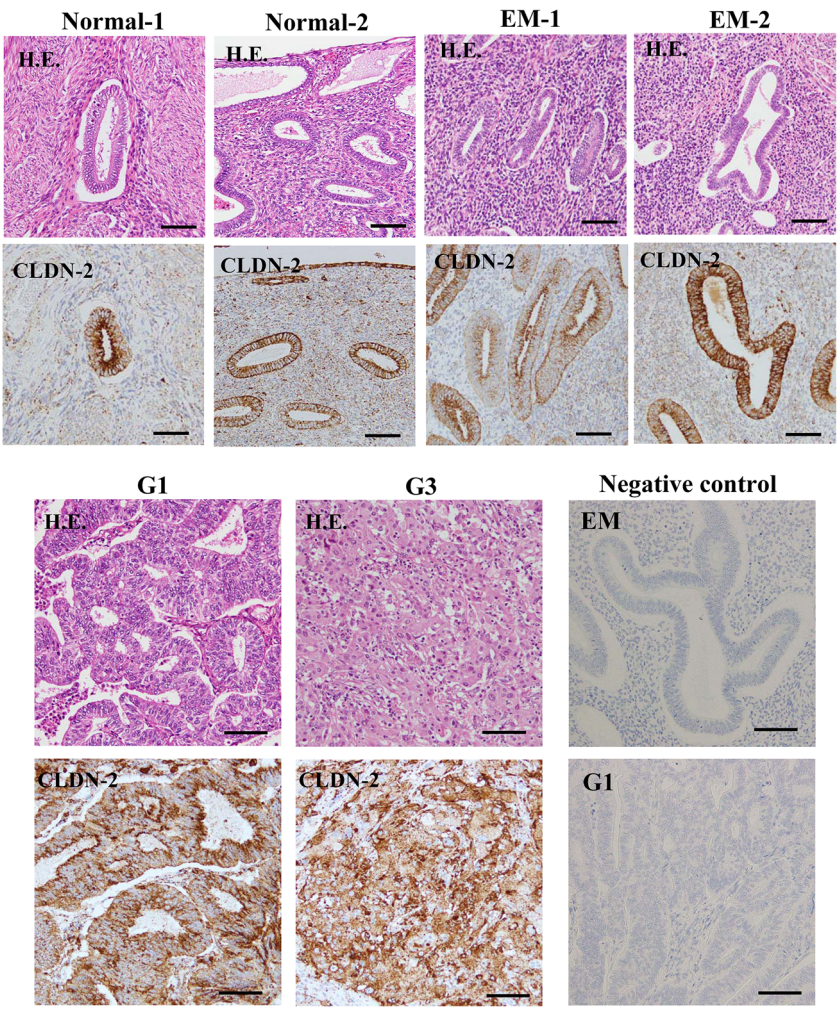

Fig. 1 Expression and distribution of CLDN-2 in normal lesions, endometriosis, and endometrioid endometrial carcinoma tissues. H.E. and immunohistochemical staining for CLDN-2 in the tissues of normal lesions (normal-1, normal-2), endometriosis (EM1, EM2), and endometrial cancer (G1, G3). Negative controls (EM, G1). Scale bar, 100 μm

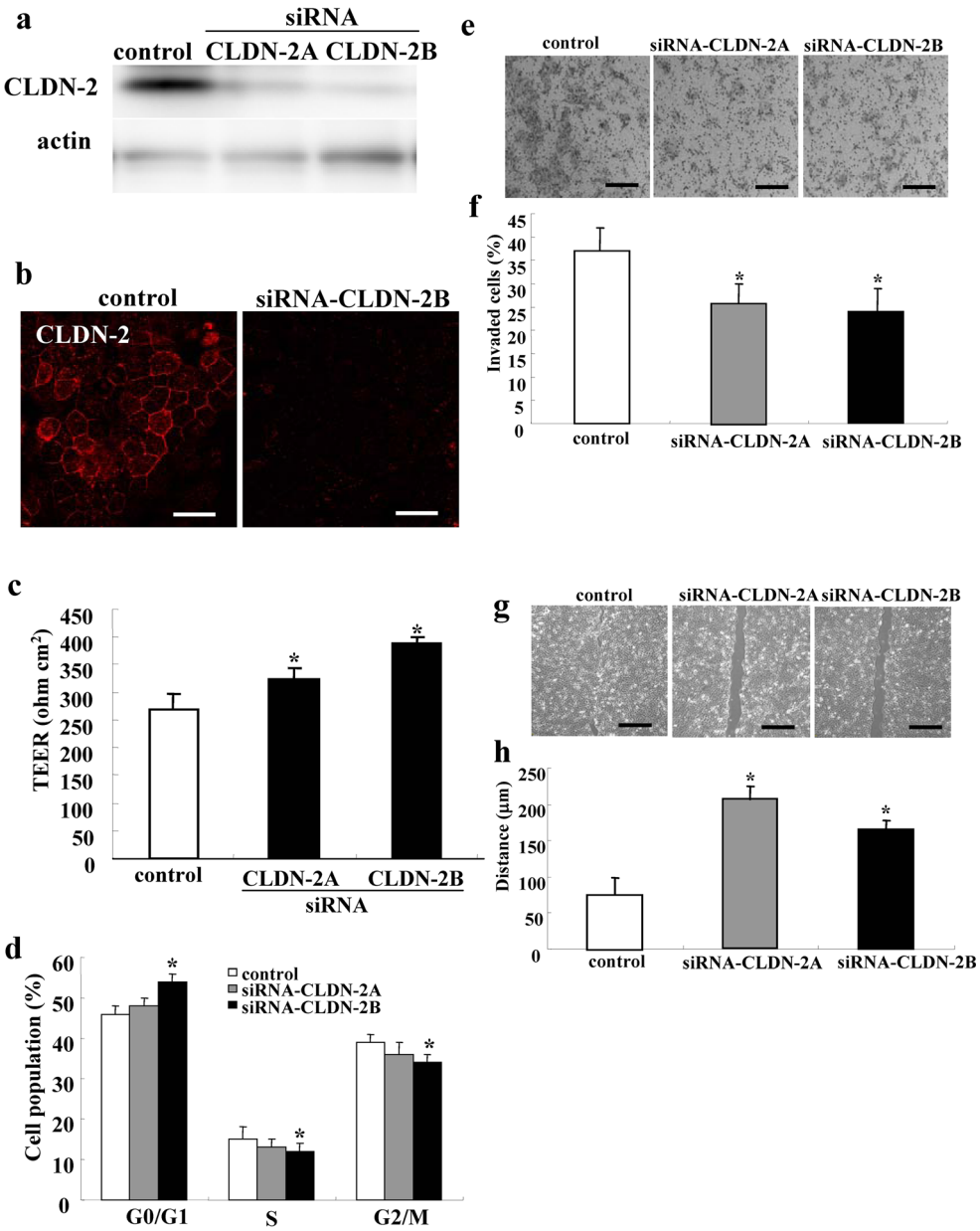

Fig. 2 Effects of CLDN-2 knockdown on barrier function, cell cycle, migration, and invasion of Sawano cells. **a** Western blotting for CLDN-2 in Sawano cells transfected with siRNAs of CLDN-2A and 2B. **b** Immunocytochemical staining for CLDN-2 in Sawano cells transfected with siRNA of CLDN-2B. Scale bar, 20 μm. **c** Bar graph TEER values representing barrier function of Sawano cells transfected with siRNAs of CLDN-2A and 2B. $p^* < 0.05$ vs control. **d** Cell cycle assay of Sawano cells transfected with siRNAs of CLDN-2A and 2B. $p^* < 0.05$ vs control. **e**, **f** Matrigel invasion assay of Sawano cells transfected with siRNAs of CLDN-2A and 2B. $p^* < 0.05$ vs control. Scale bar, 100 μm. **g**, **h** Migration assay of Sawano cells transfected with siRNAs of CLDN-2A and 2B. $p^* < 0.05$ vs control. Scale bar, 400 μm

Loss of CLDN-2 Inhibits Cell Invasion and Migration in Sawano Cells

To investigate whether loss of CLDN-2 affected cell invasion and migration in Sawano cells, we performed cell invasion and migration assay after knockdown of CLDN-2 by the siRNAs. Cell invasion and migration were significantly inhibited by siRNAs of CLDN-2A and CLDN-2B (Fig. 2e–h).

High-Glucose Condition Decreases CLDN-2 Protein and Upregulates Barrier Function in Sawano Cells

We performed GeneChip analysis of Sawano cells treated in high-glucose medium for 24 h and selected gene probes that were regulated more or less than about two-fold compared to the controls and high-glucose condition (Table 2). In the high-glucose condition,

Table 2 List of gene probes up- or downregulated in Sawano cells cultured in high-glucose medium

Gene name	ID	Gene bank ID	Fold-change control vs H-glucose
Claudin-2	H200002539	NM001171095.1	0.14
AREG	CHsGV10000152	NM001657.3	2.67

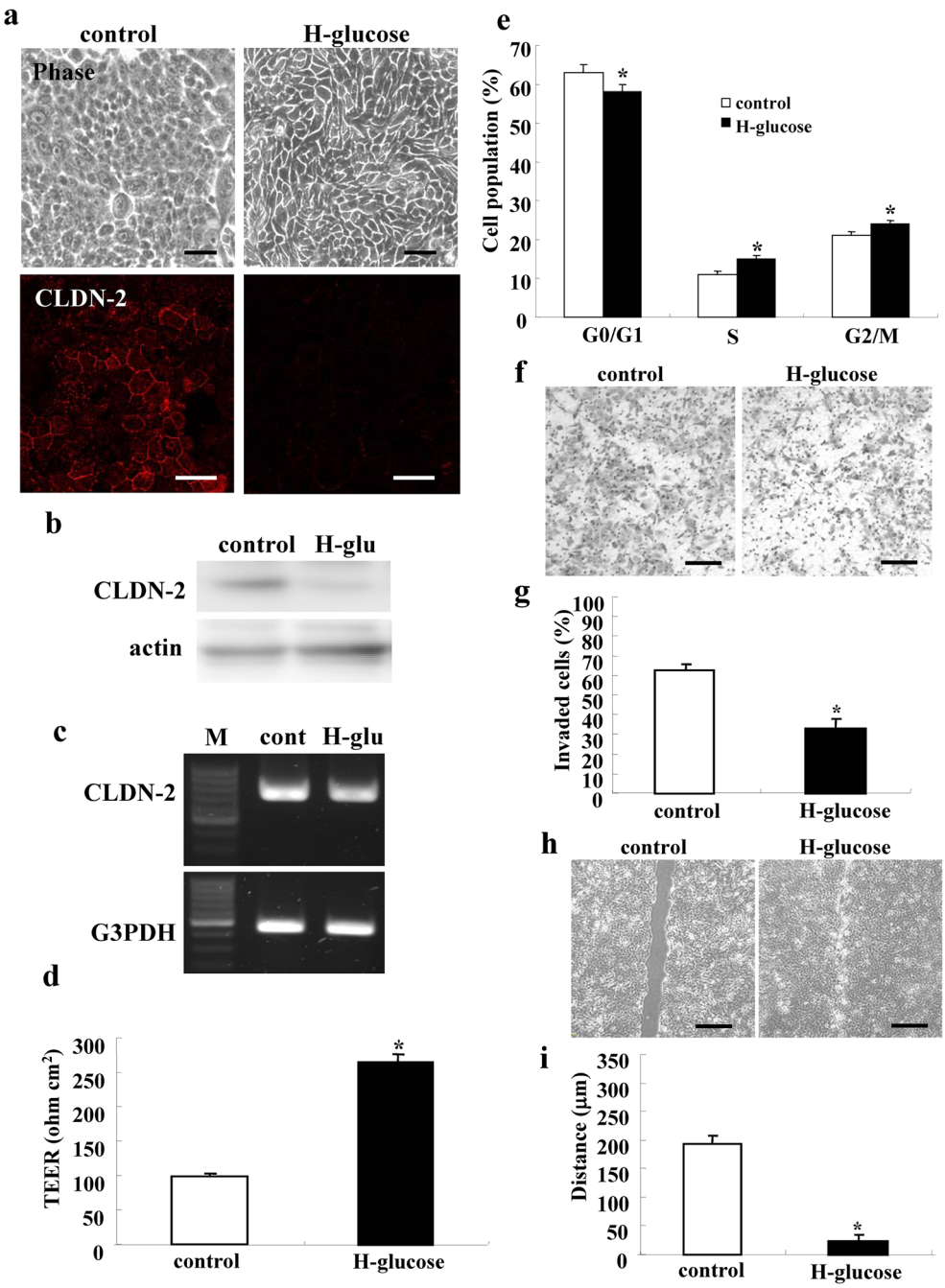

Fig. 3 Effects of high-glucose condition on CLDN-2 expression, barrier function, cell cycle, migration, and invasion of Sawano cells. **a** Phase-contrast images and immunocytochemical staining of CLDN-2 in Sawano cells treated with high-glucose medium. Scale bar of phase-contrast images, 40 μm. Scale bar of immunocytochemical staining, 20 μm. **b** Western blotting for CLDN-2 in Sawano cells treated with high-glucose medium. **c** RT-PCR for CLDN-2 in Sawano cells treated with high-glucose medium. **d** Bar graph TEER values representing barrier function of Sawano cells treated with high-glucose medium. $p^* < 0.05$ vs control. **e** Cell cycle assay of Sawano cells treated with high-glucose medium. $p^* < 0.05$ vs control. **f**, **g** Matrigel invasion assay of Sawano cells treated with high-glucose medium. $p^* < 0.05$ vs control. Scale bar, 100 μm. **h**, **i** Migration assay of Sawano cells treated with high-glucose medium. $p^* < 0.05$ vs control. Scale bar, 400 μm

downregulation of CLDN-2 and upregulation of amphregulin (AREG) were observed compared to the control. To investigate CLDN-2 regulation in endometrial cancers, Sawano cells were cultured in high-glucose medium for 24 h. In immunocytochemical and Western blotting analyses, CLDN-2 protein was decreased in the high-glucose condition (Fig. 3a, b). In RT-PCR analysis, no change of CLDN-2 mRNA was observed between the control and the high-glucose condition (Fig. 3c). In the high-glucose condition, the values of TEER were increased (Fig. 3d).

High-Glucose Condition Inhibits Cell Invasion and Induces Cell Migration and G2/M Arrest in Sawano Cells

To investigate whether the high-glucose condition affected cell proliferation, invasion, and migration in Sawano cells, we performed assays of the cell cycle, cell invasion, and cell migration after culture in high-glucose medium for 24 h. In the cell cycle assay, the G2/M and S phases were increased and the G0/G1 phase was decreased in the high-glucose condition

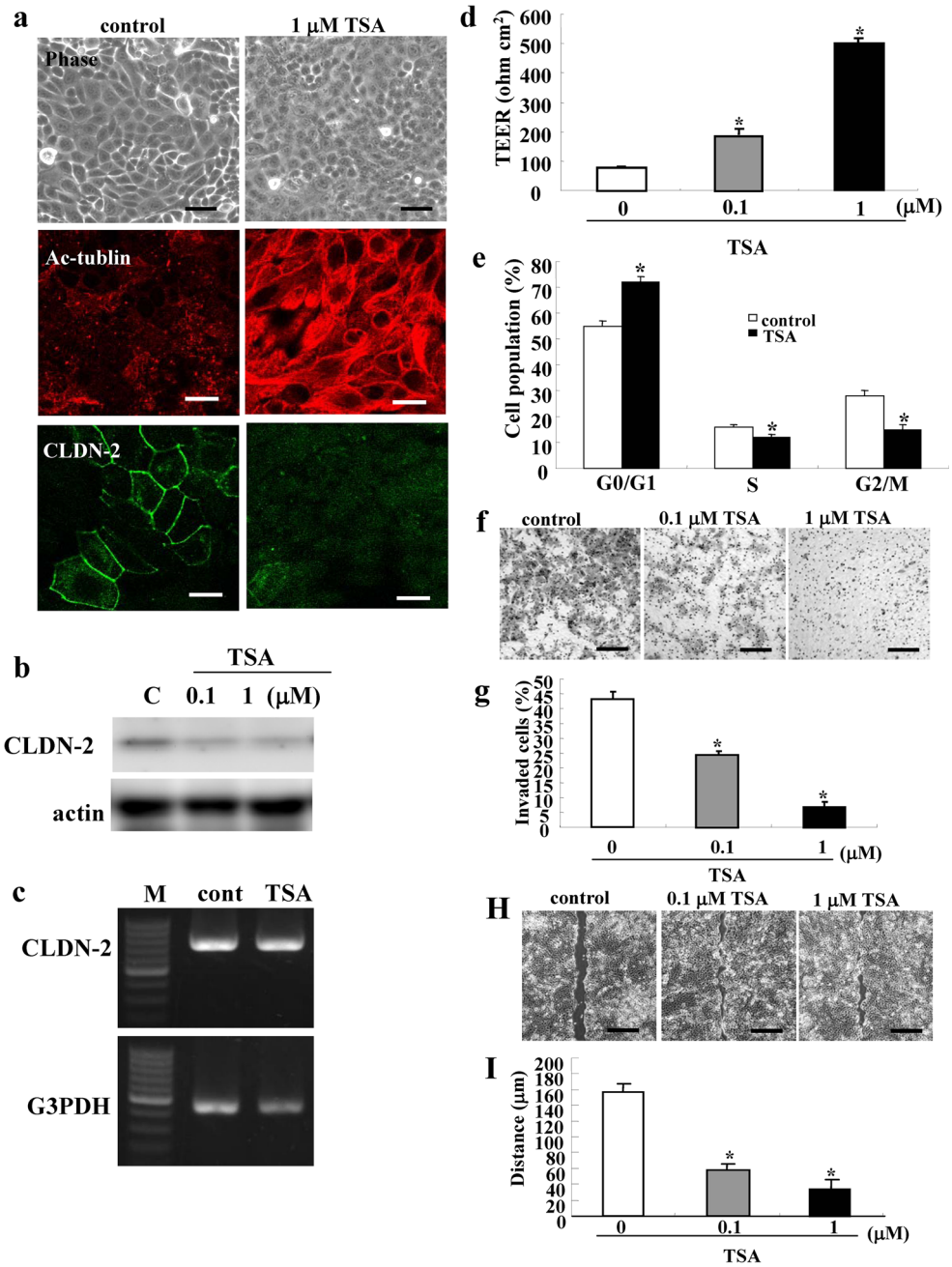

Fig. 4 Effects of trichostatin A (TSA) on CLDN-2 expression, barrier function, cell cycle, cell migration, and invasion of Sawano cells. **a** Phase-contrast images and immunocytochemical staining of CLDN-2 in Sawano cells treated with 1 μM TSA. Scale bar of phase-contrast images, 40 μm. Scale bar of immunocytochemical staining, 20 μm. **b** Western blotting for CLDN-2 in Sawano cells treated with 0.1 or 1 μM TSA. **c** RT-PCR for CLDN-2 in Sawano cells treated 1 μM TSA. **d** Bar graph TEER values representing barrier function of Sawano cells treated with 0.1 or 1 μM TSA. $p^* < 0.05$ vs control. **e** Cell cycle assay of Sawano cells treated with 1 μM TSA. $p^* < 0.05$ vs control. **f**, **g** Matrigel invasion assay of Sawano cells treated with 0.1 or 1 μM TSA. $p^* < 0.05$ vs control. Scale bar, 100 μm. **h**, **i** Migration assay of Sawano cells treated with 0.1 or 1 μM TSA. $p^* < 0.05$ vs control. Scale bar, 400 μm

(Fig. 3e). This condition inhibited cell migration and induced cell invasion (Fig. 3f–i).

HDAC Inhibitor Trichostatin A (TSA) Downregulates CLDN-2 Protein and Upregulates Barrier Function in Sawano Cells

To investigate whether CLDN-2 was regulated via HDAC in endometrial cancers, we treated Sawano cells with the HDAC inhibitor TSA at 0.1 or 1 μM for 24 h. Immunocytochemical analysis revealed that CLDN-2 was decreased and acetylated tubulin expression was increased by treatment with 1 μM TSA (Fig. 4a). In Western blot analysis, CLDN-2 protein was decreased by treatment with 0.1 and 1 μM TSA (Fig. 4b). In RT-PCR analysis, no change of CLDN-2 mRNA was observed between the control and treatment with 1 μM TSA (Fig. 4c). By treatment with TSA, the values of TEER were increased in a dose-dependent manner (Fig. 4d).

Trichostatin A (TSA) Inhibits Cell Invasion and Induces G1 Arrest and Cell Migration in Sawano Cells

To investigate whether TSA affected the cell proliferation, invasion, and migration in Sawano cells, we performed assays

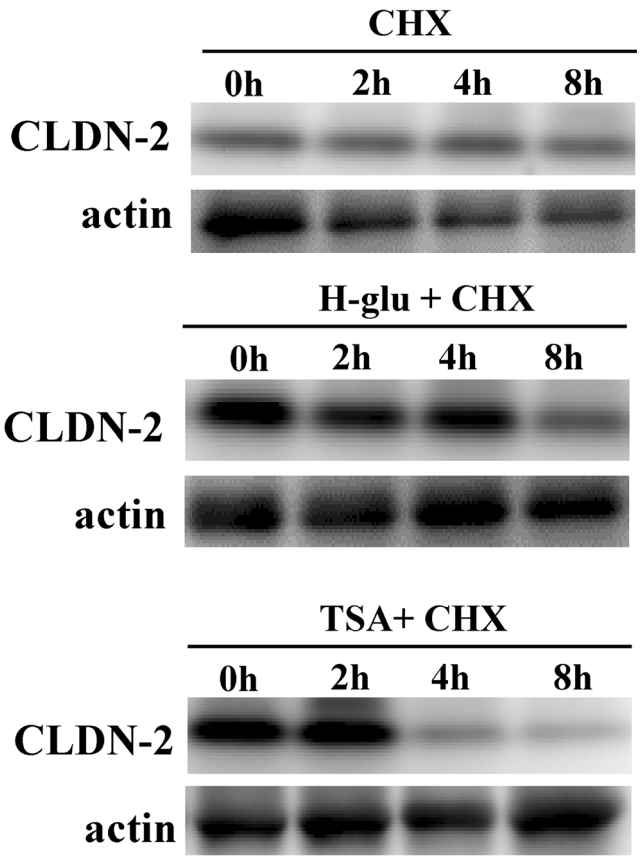

Fig. 5 Protein expression of CLDN-2 in Sawano cells treated with cycloheximide (CHX). Western blotting for CLDN-2 in Sawano cells treated with CHX with or without high-glucose medium or 1 μM TSA

of the cell cycle, cell invasion, and cell migration after treatment with TSA at 0.1 or 1 μM for 24 h. In the cell cycle assay, the G0/G1 phase was increased and the G2/M and S phases were decreased by treatment with 1 μM TSA (Fig. 4e). Treatment of TSA inhibited cell invasion and induced cell migration in a dose-dependent manner (Fig. 4f–i).

High-Glucose Condition and Trichostatin A (TSA) Induce Degradation of CLDN-2 in Sawano Cells

To elucidate the mechanism of the decrease of protein but not mRNA of CLDN-2 caused by the treatment a high-glucose concentration and TSA in Sawano cells, we examined the protein level of CLDN-2 in a time-dependent manner after treatment with 50 μM cycloheximide (a translation inhibitor) 24 h after exposure to the high-glucose condition and TSA. In the presence of cycloheximide, treatment with a high-glucose concentration and TSA enhanced the decrease of CLDN-2 in a time-dependent manner (Fig. 5). This result indicated that the high-glucose treatment and TSA might induce degradation of CLDN-2 in Sawano cells.

CLDN-2 Knockdown and High-Glucose Condition but Not Trichostatin A (TSA) Affect Mitochondrial Respiration in Sawano Cells

To investigate whether CLDN-2 knockdown, the high-glucose condition, and TSA affected mitochondrial function in the cellular metabolism, we utilized the XFe cell mito stress test assay. In the XFe cell mitochondrial stress test assay, the oxygen consumption rate (OCR) was used as an indicator of mitochondrial respiration function. Oligomycin, an ATP synthase inhibitor, was used for probing ATP production. Carbonylcyanide-4-phenylhydrazone (FCCP), an oxidative phosphorylation uncoupling agent, was used for probing maximal respiration. A mixture of rotenone and antimycin A (R + AA), inhibited complex I and complex III, resulting in complete inhibition of mitochondrial respiration, and determination of the non-mitochondrial oxygen consumption was used for calculating spare respiratory capacity (SRC) (Fig. 6d). The basal respiration and ATP production levels were not significantly altered. However, the maximal respiration and SRC levels were downregulated by CLDN-2 knockdown compared to the control in Sawano cells (Fig. 6a). The basal respiration, ATP production, maximal respiration, and SRC levels were upregulated by the high-glucose condition, and they were downregulated by the low-glucose condition compared to the control in Sawano cells (Fig. 6b). Treatment with 0.1 μM and 1 μM TSA did not significantly affect the basal respiration, ATP production, maximal respiration or SRC levels (Fig. 6c).

Discussion

In the present study, we first found that overexpression of the leaky-type tight junction protein CLDN-2 closely contributed to the malignancy of human endometrioid endometrial adenocarcinoma. Downregulation of CLDN-2 upregulated the epithelial barrier and inhibited not only cell proliferation but also cell migration and cell invasion in endometrial cancer cells.

The elevation of CLDN-2 has been reported in various cancers [11–14]. In human endometrial cancer tissues, CLDN-2 expression increased in G3 endometrioid endometrial adenocarcinoma compared to that in G1, and in endometriosis, a change in the localization of CLDN-2 was observed. These findings suggested that CLDN-2 might be involved in the malignancy of human endometrial cancer.

As CLDN-2 forms paracellular cation and water-permeable channels, overexpression and downregulation of CLDN-2 in various cell lines increase and decrease permeability, respectively [33]. Altered claudin-2 expression also affects signaling and cell behavior including proliferation, migration, and cell fate determination [33]. Claudin-2 is thought to be a pathogenic factor in several diseases due to its permeability-

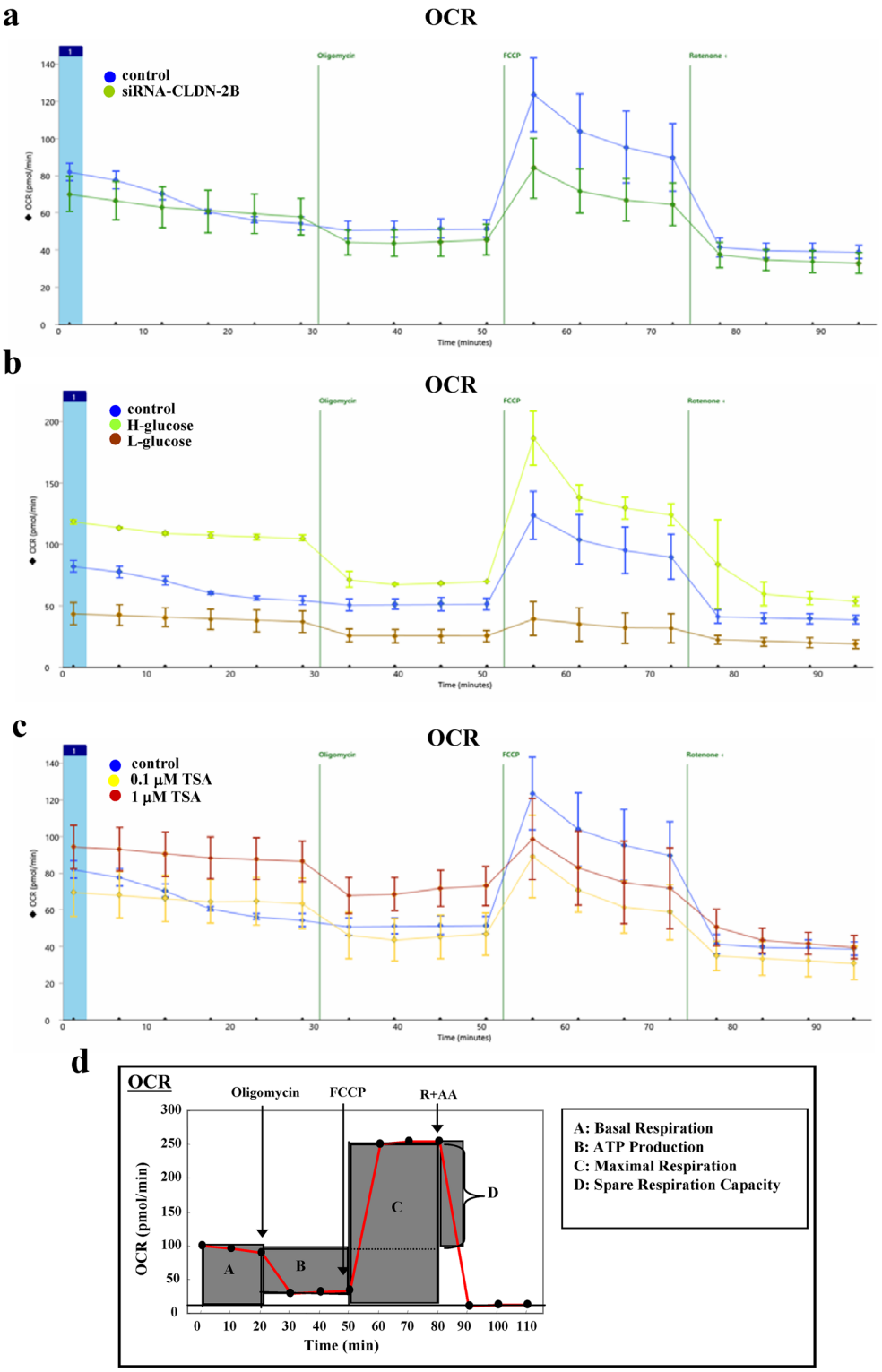

Fig. 6 Effects of CLDN-2 knockdown, high-glucose medium, low-glucose medium, and trichostatin A (TSA) on OCR in Sawano cells. **a** OCR graphs of Sawano cells transfected with siRNA-CLDN-2B. **b** OCR graphs of Sawano cells treated with high- or low-glucose medium. **c** OCR graphs of Sawano cells treated with 0.1 or 1 μM TSA. **d** Graphical explanation of OCR graph

dependent and permeability-independent functions. In the present study, downregulation of CLDN-2 increased epithelial barrier function in human endometrial cancer cells. Furthermore, downregulation of CLDN-2 induced the G0/G1 cell cycle and inhibited the G2/M cell cycle in human endometrial cancer cells. In human lung adenocarcinoma cell line A549, knockdown of CLDN-2 by siRNA decreases proliferation concomitant with suppression of cell cycle G1/S progression [15]. EGFR-ERK signaling is one of the pathways associated with G1/S cell cycle progression in cancer

cells and increases claudin-2 expression [33–35]. Therefore, it is thought that CLDN-2 expression via EGFR-ERK might affect cell proliferation in human endometrial cancer.

Furthermore, in human endometrial cancer cells, cell migration was inhibited by the knockdown of CLDN-2. Both knockdown and overexpression of CLDN-2 enhance cell migration in different cell types [33]. The effects of claudin-2 on cell migration may be involved in both cancer biology and tissue regeneration, although the mechanisms for a positive effect of claudin-2 on migration remain unclear.

Mitochondrial dysfunction may be a novel potential driver of epithelial-to-mesenchymal transition (EMT) in cancer [26], and it contributes to altered barrier permeability [28]. It is thought that mitochondrial dysfunction in type I endometrioid endometrial carcinoma contributes to tumor progression and prognosis [27]. In the present study, the mitochondrial respiration levels were downregulated by CLDN-2 knockdown in human endometrial cancer cells. It is possible that CLDN-2 expression may affect the malignancy of endometrial cancer cells via mitochondrial dysfunction.

In MDCK cells, acute and chronic exposure to high levels of glucose modulates tight junction-associated epithelial barrier function and glucose treatment induces a significant increase of CLDN-2 [21]. In the present study, the high-glucose condition decreased CLDN-2 expression, increased barrier function, and inhibited cell invasion. These results suggested that the high-glucose condition might affect barrier function and cell invasion via downregulation of CLDN-2 in human endometrial cancer cells. However, the high glucose level induced cell migration, inhibited the G0/G1 cell cycle, and induced the G2/M cell cycle in human endometrial cancer cells. The mitochondria respiration levels were upregulated in the high-glucose condition. These opposite results between the high-glucose condition and the knockdown of CLDN-2 may be explained by the difference of cell metabolism.

It is reported that the HDAC inhibitor TSA suppresses the expression of CLDN-2 in human lung adenocarcinoma cells [31]. In the present study, TSA treatment decreased CLDN-2 expression, downregulated the barrier function, induced the G0/G1 cell cycle, and inhibited the G2/M cell cycle in human endometrial cancer cells, suggesting that TSA treatment may affect the barrier function, cell cycle, and cell invasion via downregulation of CLDN-2 in human endometrial cancer cells. However, TSA treatment induced cell migration and did not significantly affect the mitochondrial respiration levels. These opposite results between TSA treatment and the knockdown of CLDN-2 may also be explained by the difference of cell metabolism.

CLDN-2 expression is modified by both transcriptional and posttranscriptional factors [33]. In the present study, decreases of protein, but not mRNA, of CLDN-2 caused by the treatment with high glucose concentration and TSA were observed in human endometrial cancer cells. In the presence of cycloheximide, the high-glucose condition and TSA enhanced the decrease of CLDN-2 in a time-dependent manner. These results indicated that treatment with a high concentration of glucose and TSA might induce degradation of CLDN-2. It is possible that overexpression of claudin-2 in endometrial cancer cells may be regulated by posttranslational modifications.

In conclusion, overexpression of CLDN-2 is involved in the malignancy of human endometrioid endometrial adenocarcinoma. Downregulation of CLDN-2 via the changes of the glucose condition and treatment with HDAC inhibitors may be important in therapy for endometrial cancer. To establish a therapy targeting CLDN-2 in human endometrial cancer, it is necessary to analyze the more detailed roles of CLDN-2 in the cancer metabolism.

Acknowledgments This work was supported by the Ministry of Education, Culture, Sports, Science, and Technology, and the Ministry of Health, Labour and Welfare of Japan.

Authors' Contributions Statement T. Okada, T. Konno and T. Kojima designed and coordinated the study and wrote the main manuscript text. T. Okada, T. Konno and T. Kojima analyzed the data. T. Kohno, H.S., S.S. and T.S. contributed reagents/materials. All authors reviewed the manuscript.

Compliance with Ethical Standards

Ethics Statement The protocol for human study was reviewed and approved by the ethics committee of Sapporo Medical University School of Medicine. Written informed consent was obtained from each patient who participated in the investigation. All experiments were carried out in accordance with the approved guidelines and the Declaration of Helsinki.

Conflict of Interest The authors declare that they have no competing interests.

References

1. Ferlay J, Soerjomataram I, Dikshit R, Eser S, Mathers C, Rebelo M, et al. Cancer incidence and mortality worldwide: sources, methods and major patterns in GLOBOCAN 2012. Int J Cancer. 2015;136(5):E359–86.
2. Lortet-Tieulent J, Ferlay J, Bray F, Jemal A. International patterns and trends in endometrial cancer incidence, 1978-2013. J Natl Cancer Inst. 2018;110(4):354–61.
3. Angelow S, Ahlstrom R, Yu AS. Biology of claudins. Am J Physiol Renal Physiol. 2008;295(4):F867–76.
4. Furuse M, Tsukita S. Claudins in occluding junctions of humans and flies. Trends Cell Biol. 2006;16(4):181–8.
5. Matter K, Balda MS. Signalling to and from tight junctions. Nat Rev Mol Cell Biol. 2003;4(3):225–36.
6. Furuse M, Fujita K, Hiiragi T, Fujimoto K, Tsukita S. Claudin-1 and -2: novel integral membrane proteins localizing at tight junctions with no sequence similarity to occludin. J Cell Biol. 1998;141(7):1539–50.
7. Tsukita S, Furuse M, Itoh M. Multifunctional strands in tight junctions. Nat Rev Mol Cell Biol. 2001;2(4):285–93.

8. Mineta K, Yamamoto Y, Yamazaki Y, Tanaka H, Tada Y, Saito K, et al. Predicted expansion of the claudin multigene family. FEBS Lett. 2011;585(4):606–12.
9. Turksen K, Troy TC. Barriers built on claudins. J Cell Sci. 2004;117(Pt 12):2435–47.
10. Leech AO, Cruz RG, Hill AD, Hopkins AM. Paradigms lost-an emerging role for over-expression of tight junction adhesion proteins in cancer pathogenesis. Ann Transl Med. 2015;3(13):184.
11. Ikari A, Sato T, Watanabe R, Yamazaki Y, Sugatani J. Increase in claudin-2 expression by an EGFR/MEK/ERK/c-Fos pathway in lung adenocarcinoma A549 cells. Biochim Biophys Acta. 2012;1823(6):1110–8.
12. Halász J, Holczbauer A, Páska C, Kovács M, Benyó G, Verebély T, et al. Claudin-1 and claudin-2 differentiate fetal and embryonal components in human hepatoblastoma. Hum Pathol. 2006;37(5): 555–61.
13. Kinugasa T, Huo Q, Higashi D, Shibaguchi H, Kuroki M, Tanaka T, et al. Selective up-regulation of claudin-1 and claudin-2 in colorectal cancer. Anticancer Res. 2007;27(6A):3729–34.
14. Xin S, Huixin C, Benchang S, Aiping B, Jinhui W, Xiaoyan L, et al. Expression of Cdx2 and claudin-2 in the multistage tissue of gastric carcinogenesis. Oncology. 2007;73(5–6):357–65.
15. Ikari A, Watanabe R, Sato T, Taga S, Shimobaba S, Yamaguchi M, et al. Nuclear distribution of claudin-2 increases cell proliferation in human lung adenocarcinoma cells. Biochim Biophys Acta. 2014;1843(9):2079–88.
16. Ikari A, Sato T, Takiguchi A, Atomi K, Yamazaki Y, Sugatani J. Claudin-2 knockdown decreases matrix metalloproteinase-9 activity and cell migration via suppression of nuclear Sp1 in A549 cells. Life Sci. 2011;88(13–14):628–33.
17. Tabariès S, Dong Z, Annis MG, Omeroglu A, Pepin F, Ouellet V, et al. Claudin-2 is selectively enriched in and promotes the formation of breast cancer liver metastases through engagement of integrin complexes. Oncogene. 2011;30(11):1318–28.
18. Friberg E, Orsini N, Mantzoros CS, Wolk A. Diabetes mellitus and risk of endometrial cancer: a meta-analysis. Diabetologia. 2007;50(7):1365–74.
19. Lacey JV Jr, Chia VM. Endometrial hyperplasia and the risk of progression to carcinoma. Maturitas. 2009;63(1):39–44.
20. Gu CJ, Xie F3, Zhang B, Yang HL, Cheng J, He YY, et al. High glucose promotes epithelial-mesenchymal transition of uterus endometrial cancer cells by increasing ER/GLUT4-mediated VEGF secretion. Cell Physiol Biochem. 2018;50(2):706–20.
21. Mongelli-Sabino BM, Canuto LP, Collares-Buzato CB. Acute and chronic exposure to high levels of glucose modulates tight junction-associated epithelial barrier function in a renal tubular cell line. Life Sci. 2017;188:149–57.
22. Sobel G, Németh J, Kiss A, Lotz G, Szabó I, Udvarhelyi N, et al. Claudin 1 differentiates endometrioid and serous papillary endometrial adenocarcinoma. Gynecol Oncol. 2006;103(2):591–8.
23. Szabó I, Kiss A, Schaff Z, Sobel G. Claudins as diagnostic and prognostic markers in gynecological cancer. Histol Histopathol. 2009;24(12):1607–15.
24. Hoerscher A, Horné F, Dietze R, Berkes E, Oehmke F, Tinneberg HR, et al. Localization of claudin-2 and claudin-3 in eutopic and ectopic endometrium is highly similar. Arch Gynecol Obstet. 2020;301(4):1003–11.
25. Cruz-Bermúdez A, Vicente-Blanco RJ, Gonzalez-Vioque E, Provencio M, Fernández-Moreno MÁ, Garesse R. Spotlight on the relevance of mtDNA in cancer. Clin Transl Oncol. 2017;19(4):409–18.
26. Guerra F, Guaragnella N, Arbini AA, Bucci C, Giannattasio S, Moro L. Mitochondrial dysfunction: a novel potential driver of epithelial-to-mesenchymal transition in cancer. Front Oncol. 2017;7:295.
27. Musicco C, Cormio G, Pesce V, Loizzi V, Cicinelli E, Resta L, et al. Mitochondrial dysfunctions in type I endometrial carcinoma: exploring their role in oncogenesis and tumor progression. Int J Mol Sci. 2018;19(7):E2076.
28. Yang L, Na CL, Luo S, Wu D, Hogan S, Huang T, et al. The phosphatidylcholine transfer protein stard7 is required for mitochondrial and epithelial cell homeostasis. Sci Rep. 2017;7:46416.
29. Garmpis N, Damaskos C, Garmpi A, Spartalis E, Kalampokas E, Kalampokas T, et al. Targeting histone deacetylases in endometrial cancer: a paradigm-shifting therapeutic strategy? Eur Rev Med Pharmacol Sci. 2018;22(4):950–60.
30. Wu Y, Starzinski-Powitz A, Guo SW. Trichostatin A, a histone deacetylase inhibitor, attenuates invasiveness and reactivates E-cadherin expression in immortalized endometriotic cells. Reprod Sci. 2007;14(4):374–82.
31. Hichino A, Okamoto M, Taga S, Akizuki R, Endo S, Matsunaga T, et al. Down-regulation of claudin-2 expression and proliferation by epigenetic inhibitors in human lung adenocarcinoma A549 cells. J Biol Chem. 2017;292(6):2411–21.
32. Okimura H, Tatsumi H, Ito F, Yamashita S, Kokabu T, Kitawaki J. Endometrioid carcinoma arising from diaphragmatic endometriosis treated with laparoscopy: a case report. J Obstet Gynaecol Res. 2018;44(5):972–27.
33. Venugopal S, Anwer S, Szászi K. Claudin-2: roles beyond permeability functions. Int J Mol Sci. 2019;20(22):E5655.
34. Massagué J. G1 cell-cycle control and cancer. Nature. 2004;432(7015):298–306.
35. Zhang W, Liu HT. MAPK signal pathways in the regulation of cell proliferation in mammalian cells. Cell Res. 2002;12(1):9–18.